Proceedings of the International Gas Turbine Congress 2003 Tokyo
November 2-7, 2003

IGTC2003Tokyo TS-065

Predictions Of A Turbulent Flow Inside A Sharp U-Curve Duct For A Turbine Blade Cooling Passage

Ryoichi S. AMANO[1] and Baojun SONG[1]

[1] Department of Mechanical Engineering
University of Wisconsin
Milwaukee, WI 53201, U.S.A.

Phone: 414-229-2345, FAX: 414-229-6958, E-mail: amano@uwm.edu

ABSTRACT

The internal cooling problem has been an issue of importance for the extending turbine blade life. This paper provides significant discovery of the improvement of simulation techniques for the flows inside a sharp U-curve duct. The finite volume difference method incorporated with the higher-order bounded interpolation scheme has been employed in the present study. For the purpose of comparison, the predictions with different turbulence models are also given. The results obtained through this research show that non-linear low-Re k-ω model and linear model produce the quite different secondary flow patterns. It is shown that the present non-linear model produces satisfactory predictions of the flow development inside the sharp U-curve duct.

NOMENCLATURE

a, c	weighted average coefficients
$C_i \ (i = 1 \sim 9)$	turbulence modeling constants in Eq. (3)
D	hydraulic diameter
k	turbulence kinetic energy
P	mean pressure
P_k	generation rate of $\overline{u_i u_j}$
R_c	radius of curvature of U-curve duct
Re	flow Reynolds number $(\equiv W_b D/\nu)$
Re_T	local Reynolds number
R_k, R_β, R_ω	model constants
S_{ij}	deformation tensor
U	mean velocity in cross duct direction
U_i	mean velocity tensor
u	velocity fluctuation in crossduct direction
$\overline{u_i u_j}$	Reynolds stress tensor
W	mean velocity in streamwise direction
w	velocity fluctuation in streamwise direction
W_b	streamwise bulk velocity
x	crossduct direction
y	direction normal to the duct symmetry plane
z	streamwise direction

Greek Symbols

$\alpha_0, \alpha_0^*, \beta$	model constants
δ_{ij}	Kronecker delta
ω	specific dissipation rate
Ω_{ij}	vorticity tensor
μ, μ_t	laminar and turbulence viscosity
ν	kinematic viscosity
Φ	transport variable

Superscript

Q, W	representation of QUICK and WACEB schemes, respectively

INTRODUCTION

To increase the efficiency and the power of modern power plant and aircraft gas turbines, designers are continually trying to raise the maximum turbine inlet temperature. Over the last decade the temperature has risen from 1500K to 1750K in some high-performance units. With this increase of the temperature only 25 percent can be attributed to improved alloys. New materials, such as ceramics, could help increase this maximum temperature even more in the future. However, most of the recent improvements in inlet temperature come from better cooling of the blades and greater

Manuscript Received on April 2, 2003

understanding of the heat transfer mechanism in the turbine blade passage (Amano, 2001). It is very common that cooling passages is used in gas turbine blade to enhance the cooling performance. Insufficiently cooled blades are subject to oxidation, creep rupture, and even melting. Due to a limited size of the blade, the cooling passages are created with more than one bend with a sharp turn. The flow inside the cooling passages with a sharp turn is featured with strong secondary flows induced by streamline curvature, mainstream separation, and attachment. The interactions between secondary flows and separation lead to very complex flow patterns. To accurately simulate these flows, both refined turbulence models and higher-order numerical schemes are indispensable.

The numerical studies on strongly curved U-duct have been carried out for years. Iacovides and Launder (1985) indicated that the wall-function approach had to be replaced by a low-Re turbulence model extending to the near-wall regions to predict the near-wall secondary flow with sufficient accuracy. Other studies (Besserman and Tanrikut, 1991; Xia and Taylor, 1993)) showed that the flow features through curved bends, even with moderate curvature, cannot be accurately simulated using the standard $k-\varepsilon$ model with the wall function approach. The main flow features and secondary multi-vortices in a mild-curved duct can be modestly captured using a low-Re turbulence models over the entire flow domain. Iacovides et al. (1996) conducted numerical investigation on the flow inside a sharp U–bend by using several different turbulence models including a high-Re $k-\varepsilon$ model with one-equation in the near-wall regions, a high-Re algebraic-stress model (ASM) with one-equation in the near-wall regions, a low-Re ASM model where the dissipation rate of turbulence is obtained algebraically within the wall viscous-sublayer, and a low-Re ASM model where the dissipation rate equation is solved over the entire flow domain. They concluded that turbulence anisotropy within the duct core and the wall viscous-sublayer has a strong influence on the flow development. Although the results they obtained with two low-Re ASM models were much improved compared with early work, the profiles in the separated region and downstream region from the reattachment point were still not satisfactory. They indicated that the second-moment closure model might be needed for more accurate predictions for such complex flows. The employment of the full Reynolds-stress transport models (RSM) has been one of the options to simulate the cooling passages in the gas turbine such as the work by Bonhoff et al. (1997) who presented the heat transfer prediction for rotating U-shaped coolant channels using RSM and demonstrated that reasonable agreement was achieved with the experimental data for averaged heat transfer rates in the first passage of the channel, while the heat transfer in the second passage was overestimated. Another example is the work by Chen et al. (1999) who also employed the RSM model for computing rotating two-pass square channels presenting accurate predictions of the three-dimensional flow and heat transfer characteristics resulting from rotation and strong curvature. However, one of the serious drawbacks of the use of RSM is that it requires a large memory size with a long CPU time to obtain reasonable results; thus is not practical for most of the industrial applications. For this reason, several researchers (Speziale, 1987; Nishizima and Yoshizawa, 1987; Shih et al., 1993) have focused on new two-equation models in which the quadratic terms of strain-rates are introduced into the stress-strain relation. These models can represent the anisotropy of Reynolds normal stresses, but do not have any effects of extra strain-rates on the shear stresses. Craft et al. (1993) proposed a non-linear $k-\varepsilon$ model and Song and Amano (1998) developed a non-linear $k-\omega$ model in which the cubic terms were introduced in the strain-stress relation in order to represent the effects of extra strain-rates on turbulence shear stresses. It was reported that the $k-\omega$ model has significant advantages over the $k-\varepsilon$ model in simulating three-dimensional geometry flows due to its possession of a superior stability property, thus stabilizing the numerical formulations. This is because the E terms and Yap correction appearing in the standard ε-equation are no longer needed in the transport equation for specific dissipation rate ω. Their study on turbulent flows with rotation and curvature also showed that the non-linear $k-\omega$ model proposed by them well predicted such flows. In the present study, the non-linear low-Re $k-\omega$ model is employed to simulate the complex flow inside the sharp U-curve duct.

It has been recognized that the first order scheme is sufficiently enough for the computations of the k and ε transport equations since the source and sink terms in their transport equations dominate in their distributions over the convection and the diffusion terms. However, many researchers like Bo et al. (1995) demonstrated that such first order numerical schemes produced very unsatisfactory results for a flow in a turned duct and concluded that it was essential to employ higher-order schemes for convection on the turbulence quantities as well as the mean flow variables. Therefore, Iacovides et al. (1996) employed a scheme based on a local oscillation-damping algorithm (Zhu and Leschziner, 1988) to discretize the governing equations. However, this scheme introduced the second-order diffusion into the regions where QUICK displays unbounded behavior. Therefore, a higher-order bounded interpolation scheme WACEB by Song et al. (1998) (weighted average coefficients ensuring boundedness) is adopted in this paper.

In the present study, the model comprised of the non-linear low-Re $k-\omega$ turbulence model and the higher-order numerical scheme, WACEB, is used to simulate the flow through a U-curve duct with the curvature $R_c/D=0.65$. In the present paper, we also represent the predictions for the curvature of 3.35. The Launder-Sharma (L-S) model (linear low-Re $k-\varepsilon$ model) was examined in the computations for the purpose of comparison. The success of the present predictions indicates that the model can be applied to the flow through a coolant passage in an actual gas turbine blade.

GOVERNING EQUATIONS

For steady-state turbulent flows, the averaged governing equations in an arbitrary coordinate system are written as follows:

To solve the above momentum equations, appropriate closure models must be provided for the Reynolds stresses. In the present study, a non-linear low-Re $k-\omega$ proposed by Song et al. (1999) is adopted. That is,

$$\frac{\partial \rho U_i}{\partial x_i} = 0 \tag{1}$$

$$\frac{\partial \rho U_i U_j}{\partial x_j} = -\frac{\partial P}{\partial x_i} + \frac{\partial}{\partial x_j}\left[\mu \frac{\partial U_i}{\partial x_j} - \rho \overline{u_i u_j}\right] \tag{2}$$

$$-\rho\overline{u_i u_j} = -\frac{2}{3}\delta_{ij}k + \mu_t\left(\frac{\partial U_i}{\partial x_j}+\frac{\partial U_j}{\partial x_i}\right) + C_1\frac{\mu_t}{\omega}\left(S_{ik}S_{kj}-\frac{1}{3}S_{kl}S_{kl}\delta_{ij}\right)$$
$$+C_2\frac{\mu_t}{\omega}\left(\Omega_{ik}S_{kj}+\Omega_{jk}S_{ki}\right)+C_3\frac{\mu_t}{\omega}\left(\Omega_{ik}\Omega_{jk}-\frac{1}{3}\Omega_{kl}\Omega_{kl}\delta_{ij}\right)$$
$$+C_4\frac{\mu_t}{\omega^2}\left(S_{ki}\Omega_{lj}+S_{kj}\Omega_{li}\right)S_{kl}+C_5\frac{\mu_t}{\omega^2}S_{ij}S_{kl}S_{kl} \qquad (3)$$
$$+C_6\frac{\mu_t}{\omega^2}S_{ij}\Omega_{kl}\Omega_{kl}+C_7\frac{\mu_t}{\omega^2}\left(S_{ik}S_{jm}S_{lm}-\frac{1}{3}S_{kl}S_{km}S_{lm}\delta_{ij}\right)$$
$$+C_8\frac{\mu_t}{\omega^2}\left(\Omega_{im}\Omega_{jl}S_{lm}-\frac{1}{3}\Omega_{kl}\Omega_{km}S_{lm}\delta_{ij}\right)$$
$$+C_9\frac{\mu_t}{\omega^2}\left(\Omega_{im}S_{jl}\Omega_{lm}+\Omega_{jm}S_{il}\Omega_{ml}+\frac{2}{3}\Omega_{kl}\Omega_{km}S_{lm}\delta_{ij}\right)$$

Turbulence viscosity is determined from,

$$\mu_t = \alpha^* k/\omega \qquad (4)$$

where k and ω are the turbulent kinetic energy and specific dissipation rate, respectively. α^* is a low-Re damping function introduced by Wilcox (1993) for a low-Re number flow near walls. The deformation and vorticity tensors are defined as:

$$S_{ij} \equiv \frac{\partial U_i}{\partial x_j}+\frac{\partial U_j}{\partial x_i}; \qquad \Omega_{ij} \equiv \frac{\partial U_i}{\partial x_j}-\frac{\partial U_j}{\partial x_i} \qquad (5)$$

The previous numerical study by Song and Amano (1998) for channel flow and curved channel flow as well as rotating channel flow shows that the optimal values for the coefficients in Eq. (3) are given in Table 1.

Table 1. Constants appearing in turbulence model.

C_1	C_2	C_3	C_4	C_5	C_6	C_7	C_8	C_9
-1	1	2.5	-10	-5	5	-10	5	-5

The equations for kinetic energy and specific dissipation rate are given as:

$$\frac{\partial \rho U_i k}{\partial x_i} = \frac{\partial}{\partial x_i}\left[\left(\mu+\sigma^*\mu_t\right)\frac{\partial k}{\partial x_i}\right]-\rho\beta^*\omega k + P_k \qquad (6)$$

$$\frac{\partial \rho U_i \omega}{\partial x_i} = \frac{\partial}{\partial x_i}\left[\left(\mu+\sigma\mu_t\right)\frac{\partial \omega}{\partial x_i}\right]-\rho\beta\omega^2 + \alpha\frac{\omega}{k}\mu_t S_{ij}S_{ij} \qquad (7)$$

where P_k denotes the turbulence production term and is defined as

$$P_k \equiv -\rho\overline{u_i u_j}\frac{\partial U_i}{\partial x_j}$$

and

$$\alpha^* = \frac{\alpha_0^* + \mathrm{Re}_T/R_k}{1+\mathrm{Re}_T/R_k}, \quad \alpha = \frac{5}{9}\frac{\alpha_0+\mathrm{Re}_T/R_\omega}{1+\mathrm{Re}_T/R_\omega}\left(\alpha^*\right)^{-1},$$
$$\beta^* = \frac{9}{100}\frac{5/18+\left(\mathrm{Re}_T/R_\beta\right)^4}{1+\left(\mathrm{Re}_T/R_\beta\right)^4}$$

where the constants are given in Table 2.

At the wall boundary, specific dissipation rate ω is given as

$$\omega = \frac{2\mu}{\rho\beta^* y^2} \qquad for \quad y^+ \to 0 \,(\text{smooth wall}) \qquad (8)$$

where y denotes normal distance away from the wall. Here, care must be taken to accurately compute ω through the viscous sublayer. Wilcox (1993) recommended that the first 7~10 grid points must be located in the viscous sublayer ($y^+ \le 2.5$).

Table 2. Constants appearing in turbulence model

$\sigma = \sigma^*$	β	α_0^*	α_0	R_β	R_k	R_ω
0.5	3/40	1/40	1/10	8	6	27/10

NUMERICAL METHOD

In the present work, the governing equations in a general curvilinear coordinate system are discretized by using the non-staggered finite-volume method. The coupling of the pressure and velocity is achieved through the SIMPLE algorithm (Patankar, 1980). A special interpolation procedure developed by Rhie and Chow (1987) is employed in which the flux flowing through a control volume surface is linked with the pressure at the neighboring nodes to prevent numerical oscillations which arise from decoupling of pressure gradient and velocities due to a non-staggered grid arrangement.

The numerical studies (Song et al., 1998 and Bo et al., 1995) showed that the higher-order numerical schemes should be applied in simulating complex flows in order to obtain the reliable and accurate results. In the present paper, a higher-order bounded scheme, WACEB, developed by Song *et al* (1999) is employed for computations.

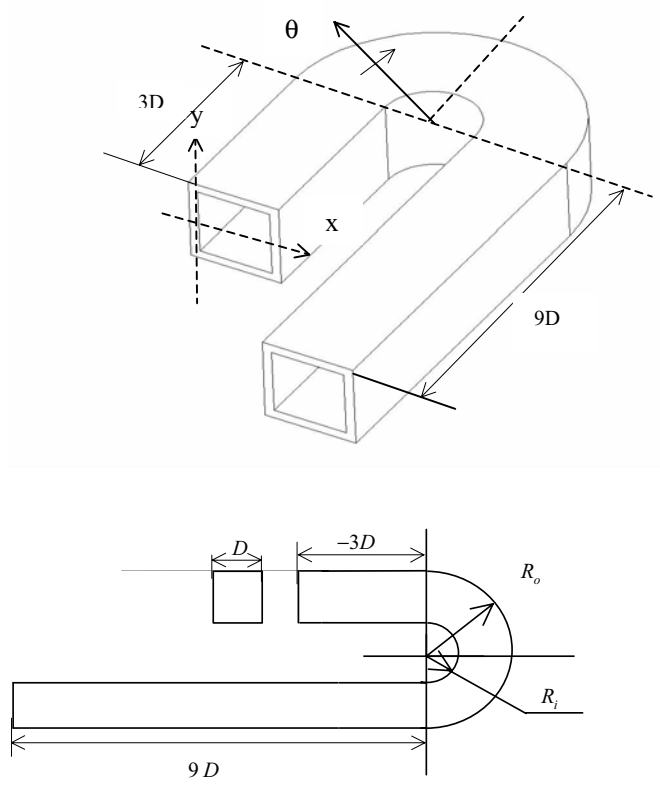

Figure 1. U-bend geometry

NUMERICAL RESULTS

The turbulent flow through a square-sectioned U-curve duct with a curvature ratio $R_c/D = 0.65$, as shown schematically in Fig. 1, is numerically simulated in the present study by using the non-linear $k-\omega$ model. The flow Reynolds number based on the hydraulic diameter and bulk velocity is 100,000. The experimental study was carried out by Cheah et al., (1994). Only the flow in the one half of the duct is computed because of the symmetry of flow configuration. The inlet conditions at three diameters upstream of the bend entry, which best matched the available measurements, were generated from separate calculations of developing flow in a straight duct that has the same mean-flow Reynolds number as in the experiment and assigned here. At the duct exit which is located at nine diameters downstream from the bend exit, the zero-gradients for velocities and turbulent quantities were employed.

On the cross-sectional plane, a non-uniform grid of 97×50 in the normal and radial directions was employed, with mesh refined in the near-wall region, as shown in Fig. 2. In the stream-wise direction, 150 stream-wise planes were used, consisting of 20 planes in the upstream sections, 70 planes within the bend, and 60 planes downstream. The grid sensitivity tests of Bo et al. (1995) showed that, provided that a higher-order scheme (LODA) was used for the discretization of all the transport equations, these grids were sufficiently fine to prevent numerical errors from deteriorating the solutions. In the present study, the first eight grid-points near the walls are located within the viscous layer $(y^+ \le 2.5)$.

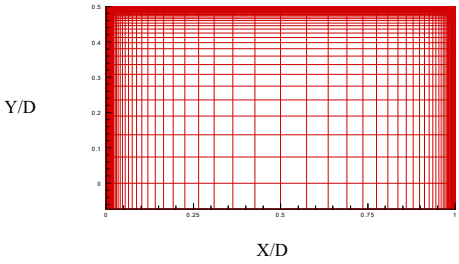

Figure. 2 Numerical grids.

The predicted mainstream velocity profiles along the symmetrical plane are shown in Fig. 3 and compared with the experimental data (Cheah et al., 1994). The results computed by using Launder-Sharma model are also included in the figure. It is observed that the flow is strongly accelerated along the inner wall from the bend entry ($\theta = 0^o$) to the plane $\theta = 45^o$, while the flow is decelerated along the outer wall due to the centrifugal forces induced by curvature. Because of the strong acceleration, the separation occurs at the $\theta = 90^o$ plane near the inner wall. Then the separation bubble grows wider, which in turn results in the flow along the outer wall accelerating. The separation bubble reaches to its maximum width in the plane $z = 1D$ downstream from the bend exit. In the plane $z = 3D$, the flow reattaches to the inner wall and recovery process begins. Comparing with the experimental data (Cheah et al., 1994), it is noticed that the present model well reproduces the flow development pattern and produces the satisfactory results. It is observed that the predicted results by using the Launder-Sharma model are less satisfactory. It is clearly seen that the Launder-Sharma model produced a narrower and longer separation bubble than the non-linear $k-\omega$ model did. It can be concluded that the present low-Re *k-* model has ability to represent the influence of turbulence anisotropy within the duct core and wall sublayer on the flow development by strong curvature. It is also noticed that the velocity profile at the plane $z = 3D$ is a little unsatisfactory, which means the predicted recovery after reattachment is a subtle slower than experiment data (note that the results with the linear Launder-Sharma model are even worse).
It is suggested that the further improvement on the model after reattachment is needed. The predicted mainstream velocity contours are illustrated in Fig. 4. From the planes $\theta = 0^o$ to $\theta = 90^o$, the variation of the mainstream velocity along y-direction is mainly limited by the near bottom-wall regions. In the plane $\theta = 90^o$, the separation in the near-wall occurs near the symmetrical plane. In the separated regions, the flow exhibits very complex three-dimensionality. The separation bubble squeezes the fluid to outer wall and the secondary flow induced by the centrifugal forces carries high momentum fluids from the duct core to the outer wall regions, which all cause the flow along the outer wall to be accelerated. Beyond the plane $z = 3D$, the three-dimensionality strongly remains. It is noted that the significant difference exists between the predictions by using the non-linear $k-\omega$ model and Launder-Sharma model.

The distributions of the cross-duct velocity (secondary velocity) component are compared with the experimental data in Fig. 5 along the symmetrical plane. The positive velocities at the bend entry $\theta = 0^o$ indicate that a strong inward motion at the bend entry is well predicted by using the present $k-\omega$ model. But it is quite uncertain why the discrepancy in the magnitude of the velocity between the prediction and the experimental data is so distinctive, although the computed trend faithfully simulates the experimental data. The calculations of Iacovides et al. (1996) showed that the four models including two low-Re ASM models all produced much lower outward velocities. In this figure, it is seen that the present model gives very satisfactory radial velocity distributions. It is also noticed that in the separated regions of the plane $\theta = 180^o$, the radial velocity is higher than the experimental data, which is consistent with the mainstream velocity profile (lower separated velocities) in this plane.

Figure 6 shows the comparisons of turbulence normal stresses between predictions and measurements in the streamwise along the symmetrical plane. The predicted turbulence normal stresses agree well with the experimental data near the outer wall. It is seen that the present model produces the quite promising profiles for normal stresses near the inner wall and separated regions, which are very similar to experimental data. However, it has to be pointed that notable discrepancies are still present.

CONCLUSIONS

In this study, the non-linear $k-\omega$, the low-Reynolds number (L-S) model as well as the higher-order bounded interpolation scheme (WACEB) has been employed to simulate the complex three-dimensional turbulent flow inside the U-curve duct with a sharp curvature. The comparisons between predicted results and experimental data show that the present non-linear model can well produce the flow development inside the U-curve duct. Compared with the linear Launder-Sharma model, it suggests that the present non-linear model well captures the characteristics of the turbulence anisotropy within the duct core region and wall sublayer and then leads to satisfactory simulations of flow development inside the U-curve duct. However, none of the turbulence models can predict turbulence quantities properly beyond the reattachment.

ACKNOWLEDGMENTS

All the computations were performed in ORIGIN 2000 at National Center for Supercomputing Applications (NCSA) in Illinois. The fund for the present project is provided by NSF under grant CTS970014N.

REFERENCES

Amano, R.S., 2001, Chapter 6: Heat transfer predictions of stator/rotor blades, *Heat transfer in Gas Turbine Blades, WIT Press.*.

Besserman, D. L., and Tanrikut, 1991, "Comparison of Heat Transfer Measurements with Computations for Turbulent Flow Around a 180Deg. Bend," *Proc. Int Gas Turbine Aeroengin Congress and Exposition* (ASME paper no. 91-G-2) Orlando, FL.

Bo, T., Iacovides, H., and Launder, B.E., 1995, "Convective Discretization Schemes for the Turbulence Transport Equations in Flow Predictions through Sharp U-Bends," *Int. J. Num. Meth. Heat Fluid Flow*, **5**, 33-48.

Bonhoff, B., Tomm, U., Johnson, B. V., and Jennions, I., 1997, "Heat Transfer Predictions for Rotating U-Shaped Coolant Channels with Skewed Ribs And with Smooth Walls," ASME 97-G-162.

Cheah, S. C., Iacovides, H., Jackson, D. C., Ji, H., and Launder, B. E., 1994, "LDA Investigation of the Flow Development through Rotating U-ducts," *Proc. Int. Gas-Turbine Congress and Exposition.* (ASME paper no. 94-GT-226) the Hague

Chen, H. C., Jang, Y. J., and Han, J. C., 1999, "Computation of Flow and Heat Transfer in Rotating Two-Pass Square Channels by a Reynolds Stress Model. ASME 99-GT-174.

Craft, T. J., Launder, B. E., and Suga, K., 1993, "Extending the Applicability of Eddy Viscosity Models through the Use of Deformation Invariants and Non-linear Elements," *Proc. 5th Symp. Refined Flow Modelling and Turbulence Measurements*, 125-132

Iacovides, H., and Launder, B. E., 1985, "ASM Predictions of Turbulent Momentum and Heat Transfer in Coils and U-Bends," *Proc. 4th int. Conference Numerical Methods Laminar and Turbulent flow*, Swansea, Wales

Iacovides, H., Launder, B. E., and Li, H., 1996, "The Computation of Flow Development through Stationary and Rotating U-Ducts of Strong Curvature," *Int. J. Heat and Fluid Flow*, **17** 22-33.

Khosla, P.K., and Rubin, S. G., 1974, "A Diagonally Dominant Second-Order Accurate Implicit Scheme," *Comput. & Fluids,* **2** 207-209.

Launder, B. E., and Sharma, B. I., 1974, "Application of the Energy-Dissipation Model of Turbulence to the Calculation of Flow near a Spinning Disc," *Letters in Heat Mass Transfer*, **1**, 131-138

Leonard, B. P., 1979, "A Stable and Accurate Convective Modeling Procedure Based on Quadratic Upstream Interpolation," *Comput. Meth. Appl. Mech. Eng,* **19**, 59-98.

Nisizima, S., and Yoshizawa, A., 1987, "Turbulent Channel Flow and Couette Flows Using an Anisotropic $k-\varepsilon$ Model," *AIAA, J.*, **25-3**, 414-420.

Patankar, S. V., 1980, *Numerical Heat Transfer and Fluid Flow*, McGraw-Hill, New York.

Rhie, C. M., and Chow, W. L., 1983 "A Numerical Study of the Turbulent Flow Past an Isolated Airfoil with Trailing Edge Separation," *AIAA J.* **21** 1525-1532.

Sathyamurthy, P. S., Karki, K. C., and Patankar, S.V., 1994, "Prediction of Turbulent Flow and Heat Transfer in a Rotating Square Duct with a 180 Deg. Bend," ASME paper 94-GT-197.

Shih, T.H., Zhu, J., and Lumley, J.L., 1993, "A Realizable Reynolds Stress Algebraic Equation Model," *NASA Technical Memorandum*, 10593.

Song, B., Liu, G. R., Lam, K. Y., and Amano, R. S., 1999, "On a Higher-Order Bounded Discretization Scheme," *Int. J. Num. Meth. Heat Fluid Flow* (in press)

Song, B., and Amano, R. S., 1998, "On Complex Turbulent Flow by Using Non-linear $k-\omega$ Model," *ASME IMECE,* Anaheim, CA

Song, B, Liu, G.R., and Amano, R.S.,2001, "Applications of a Higher-Order Bounded Numerical Scheme to Turbulent Flows," *International Journal for Numerical Methods in Fluids,* Vol. 35, pp. 371-394.

Speziale, C. G., 1987 "On Nonlinear $k-l$ and k-ω Models of Turbulence," *J. Fluid Mech.,* **178,** 459-475.

Stephens, M. A., Shih, T. I. P., and Civinskas, K. C., 1996, "Computations of Flow and Heat Transfer in a Rotating Square Duct with Smooth Walls," AIAA paper 96-3161.

Xia, J. Y., and Taylor, C., 1993, "The Prediction of Turbulent Flow and Heat Transfer in a Tight Square Sectioned 180Deg Bend," *Proc. 8th Int. Conference Numerical Methods Laminar and Turbulent Flow*, Swansea, Wales

Zhu, J., and Leschziner, M. A., 1988, "A Local Oscillation-Damping Algorithm for Higher-Order Convection Schemes," *Comput. Meth. Appl. Mech. Eng.,* **67**, 355-366.

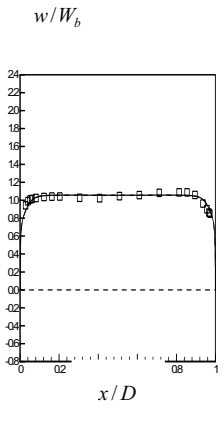

(a) Z=-3D

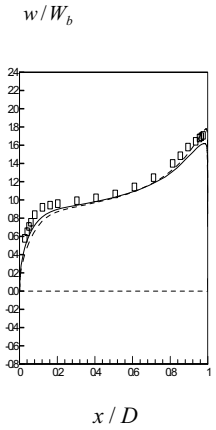

(b) θ=0°

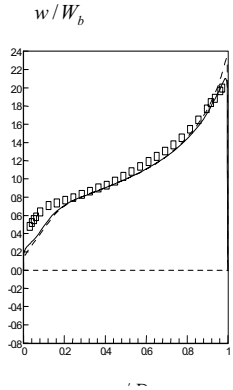

(c) θ=45°

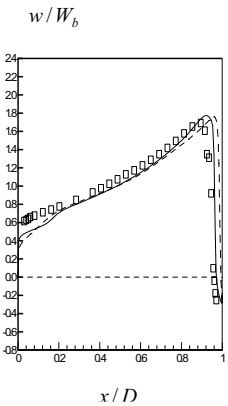

(d) θ=90°

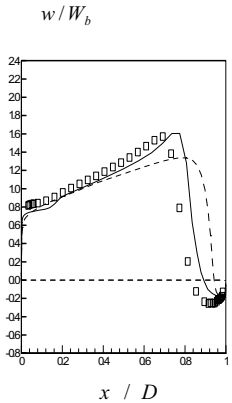

(e) θ=135°

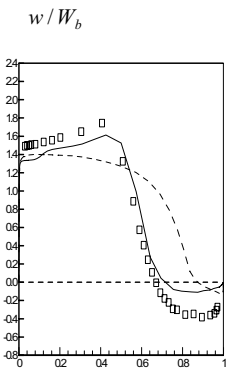

(f) θ=180°

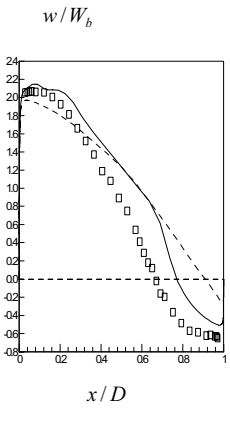

(g) $z = 1D$

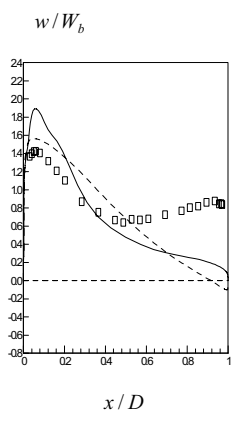

(h) $z = 1D$

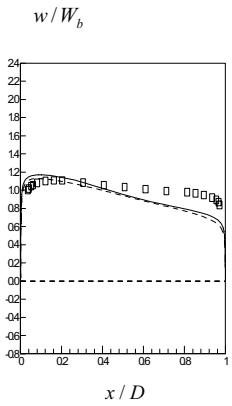

(i) $z = 3D$

Figure 3. Mainstream velocity profiles along symmetrical plane (Square symbols, Cheah et al. (1994); Solid line, present calculation with non-linear $k-\omega$ model; Dashed line, present calculation with Launder-Sharma model.

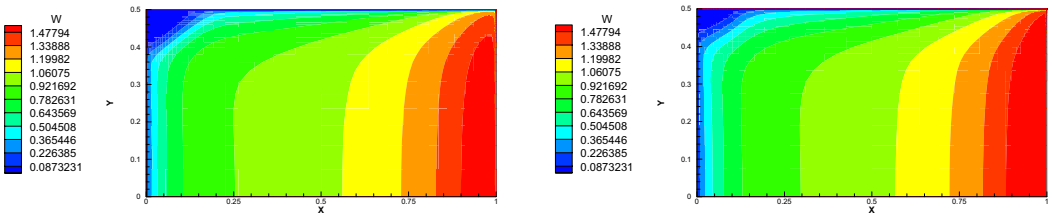

$\theta = 0^o$

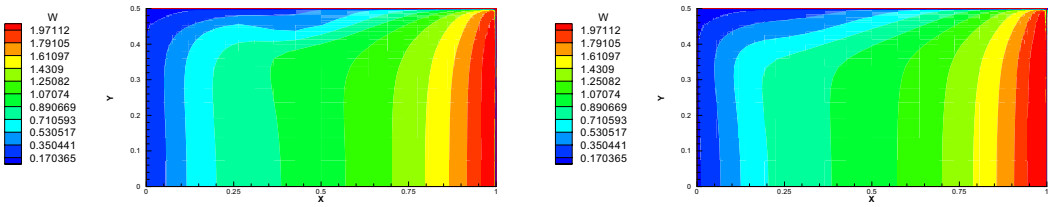

$\theta = 45^o$

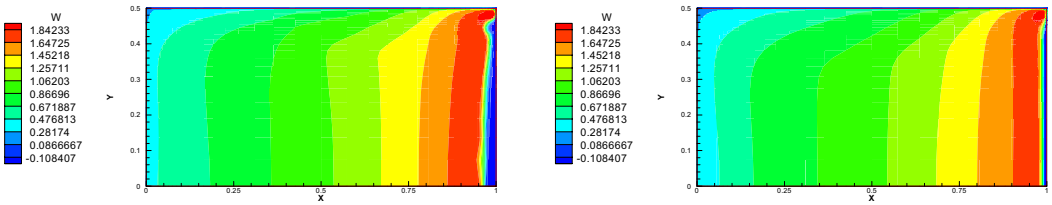

$\theta = 90^o$

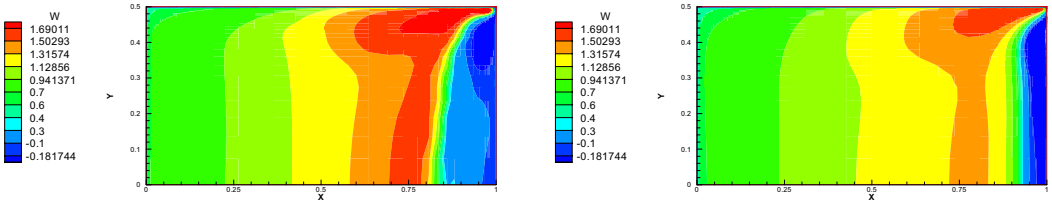

$\theta = 135^o$

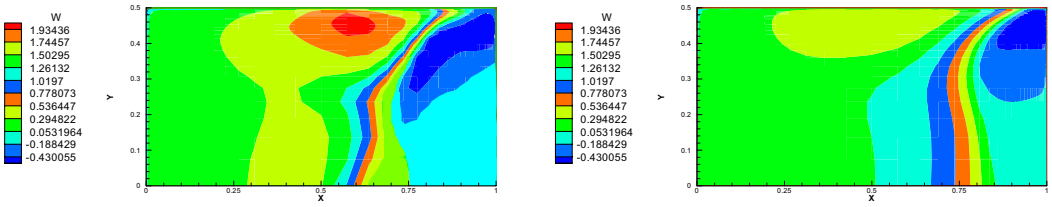

$\theta = 180^o$

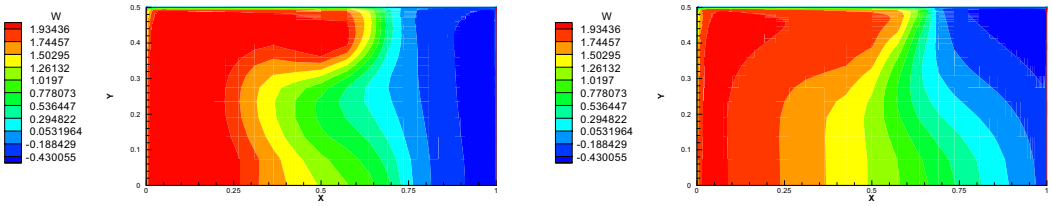

$z = 1D$

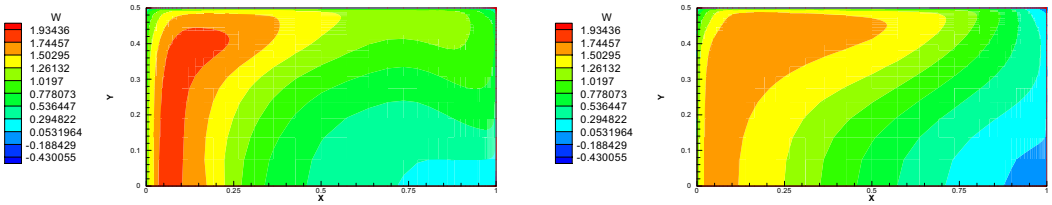

$z = 3D$

Figure 4. Predicted mainstream velocity contours (Left: non-linear $k-\omega$ model; Right low-Re k-ε model) for Rc/D=0.65.

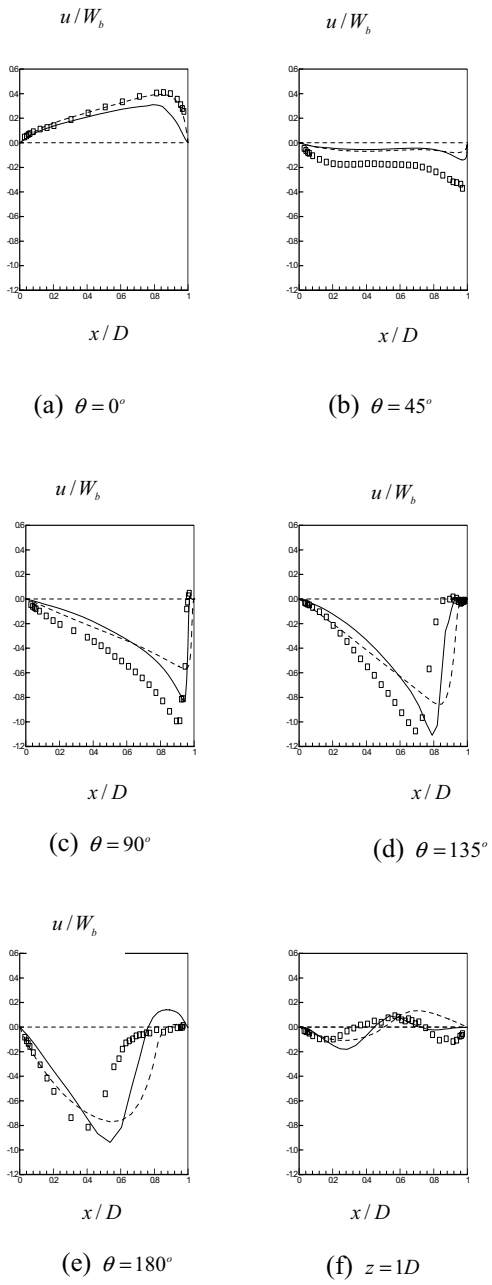

Figure 5. Secondary velocity profiles along the symmetrical plane (Square Symbols, Cheah et al. 1994; Solid line, present calculation with non-linear $k-\omega$ model; Dashed line, present calculation with Launder-Sharma model.

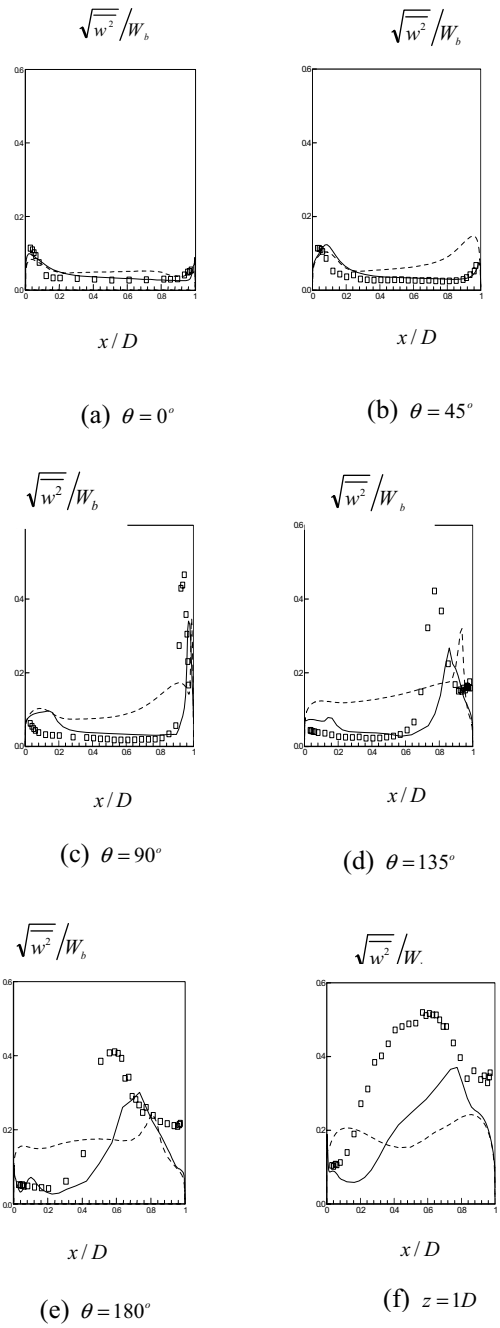

Figure 6. Reynolds stress profiles along the symmetrical plane. (Square symbols, Cheah et al. (1994); Solid line, present calculation with non-linear $k-\omega$ model; Dashed line, present calculation with Launder-Sharma model.